Veinal–mesophyll interaction under biotic stress

Michał Nosek[a], Piotr Rozpądek[c,d], Andrzej Kornaś[a], Elżbieta Kuźniak[b], Annegret Schmitt[e], Zbigniew Miszalski[d,f,*]

[a] Institute of Biology, Pedagogical University, Podchorążych 2, 30-084 Kraków, Poland
[b] Department of Plant Physiology and Biochemistry, Faculty of Biology and Environmental Protection, University of Lodz, Banacha 12/16, 90-237 Łódź, Poland
[c] Institute of Environmental Science, Jagiellonian University, Gronostajowa 7a, 30-387 Kraków, Poland
[d] Institute of Plant Physiology, Polish Academy of Sciences, Niezapominajek 21, 30-239 Kraków, Poland
[e] Julius Kühn Institute, Federal Research Institute for Cultivated Plants (JKI), Heinrichstraße 243, D-64287 Darmstadt, Germany
[f] Małopolska Centre of Biotechnology, Jagiellonian University, Gronostajowa 7a, 30-387 Kraków, Poland

ARTICLE INFO

ABSTRACT

According to microscopic observations, germinating hyphae of Botrytis cinerea, though easily penetrating Mesembryanthemum crystallinum mesophyll tissue, are limited in growth in mid-ribs and only occasionally reach vascular bundles. In mid-ribs of C_3 and CAM leaves, we found significantly lower rbcL (large RubisCO subunit) abundance. Moreover, in CAM leaves, minute transcript contents for pepc1 (phosphoenolpyruvate carboxylase) and nadpme1 (malic enzyme) genes found in the mid-ribs suggest that they perform β-carboxylation at a low rate. The gene of the main H_2O_2-scavenging enzyme, catL (catalase), showed lower expression in C_3 mid-rib parts in comparison to mesophyll. This allows maintenance of higher H_2O_2 quantities in mid-rib parts. In C_3 leaves, pathogen infection does not impact photosynthesis. However, in CAM plants, the expression profiles of rbcL and nadpme1 were similar under biotic stress, with transcript down-regulation in mid-ribs and up-regulation in mesophyll (however, in case of rbcL not significant). After B. cinerea infection in C_3 plants, transcripts for both antioxidative proteins strongly increased in mid-ribs, but not in mesophyll. In infected CAM plants, a significant transcript increase in the mesophyll was parallel to its decrease in the mid-rib region (however, in the case of catL this was not significant). Pathogen infection modified the expression of carbon and ROS metabolism genes in mid-ribs and mesophyll, resulting in the establishment of successful leaf defense.

© 2015 Elsevier GmbH. All rights reserved.

1. Introduction

Communication among leaves, stems and roots is important for integrating the whole plant response to stresses. Recently, the role of the plant vascular system as an effective long-distance communication system involved in the integration of stress response was proposed (Gorecka et al., 2015; Kocurek et al., 2015). The tissue exposed to stress can initiate and transduce stress signals to distant unaffected plant parts (Karpinski et al., 1999; Szechyńska-Hebda et al., 2010). In leaves, a layer of cells surrounding the leaf vascular tissue plays a significant role in a signal transduction between plant organs (Leegood 2008).

Plants performing β-carboxylation (C_4, CAM) at a high rate are often more resistant to different stresses,s including exogenously applied oxidative stress compared to C_3 plants (Miszalski et al., 1997; Sage 2004). It is also worth noting that some β-carboxylation-related enzymes, such as NADP-ME, are indicative of the appearance of stress (Casati et al., 1999; Dodd et al., 2002; Lüttge 2004).

Mesembryanthemum crystallinum L. (common ice plant) has been a good model comparing C_3 and β-carboxylating plants. In our earlier studies, we have shown higher sensitivity of C_3 than CAM-performing M. crystallinum plants to the necrotrophic fungus, Botrytis cinerea (Kuźniak et al., 2010, 2011; Libik-Konieczny et al., 2011). We have also found that C_3 and CAM plants respond to B. cinerea with HR-like response, but fungal growth is more limited in CAM-performing plants (Kuźniak et al., 2010). Our experimental results on the M. crystallinum–B. cinerea model system also point out that plant resistance and HR-like (Hypersensitive Response) lesions are related to H_2O_2 accumulation (Kuźniak et al., 2010). Moreover, mechanisms regulating NADP-ME (NADP-dependent malic enzyme) activity responded differently to pathogen infection in C_3- and CAM-performing plants (Libik-Konieczny et al., 2012).

* Corresponding author. Fax: +48 12 425 18 44.

In earlier studies, we have found that *M. crystallinum* vascular bundles accumulating high concentrations of malate (Ślesak et al., 2008) limit the growth of *B. cinerea* and *Pseudomonas syringae* (Kuźniak et al., 2010; Libik-Konieczny et al., 2011). Moreover, mesophyll and mid-ribs (veinal tissues) differed in the activity and content of agents involved in stress protection (Ślesak et al., 2008). To dissect whether the metabolic profile of leaf cells may determine their response to pathogen infection, we analyzed the expression of genes related to carbon metabolism [*rbcL* (large RubisCO subunit), *pepc1* (phospho*enol*pyruvate carboxylase), *nadpme* (malic enzymes)] and control of reactive oxygen species [*catL* (catalase), *cAPX1* (cytosolic ascorbate peroxidase)] in mesophyll cells and mid-ribs of *M. crystallinum* leaves infected by *B. cinerea*, as well some photochemical parameters.

2. Material and methods

2.1. Plant material

Common ice plants (*M. crystallinum*) were grown from seeds in a pot culture in a greenhouse under irradiance of 200–400 μmol quanta m^{-2} s^{-1} (PAR), photoperiod 16/8 h (day/night), temperature 27–29/17 °C and 50/80% relative humidity (RH). CAM was confirmed in NaCl-treated plants by estimation of diurnal Δmalate (diurnal malate fluctuations in the range of 10–15 mM) in the leaf cell sap with a reflectometer (RQflex 10, Merck$^{\circledR}$), according to the manufacturer's instruction.

2.2. Pathogen

The inoculation suspension was prepared according to the procedure previously described by Kuźniak et al. (2010). Inoculated plants were cultivated/grown under greenhouse conditions described above. To minimize the possible interference with the daytime fluctuations of CAM metabolism the plants were inoculated at 12:00 p.m. (phase III of CAM). All analyses were performed 48 h post-inoculation (hpi).

2.3. Gene expression analysis

Total RNA was extracted from *M. crystallinum* leaves frozen in liquid nitrogen with the Bio-rad (US) Aurum Total RNA isolation kit according to the manufacturer's instructions. Reverse transcription was carried out with 500 ng of total DNAse (DNA free kit, Ambion Bioscience US) treated RNA with iScript cDNA synthesis kit (Bio-rad, US).

For *q*PCR, probes were labeled with the EVAGreen (SsoFastEvaGreenSupermix, Bio-rad, US) fluorescent dye. For a single reaction 0.5 μl of cDNA and 150 nM of gene specific primers were used. To test amplification specificity a dissociation curve was acquired by heating samples from 60 °C to 95 °C. As house-keeping reference polyubiquitin (gi|327492448) was used. Left primer sequence: GCACCTTGGCTGACTACAAT, right primer sequence: ACCGAGTTCATCCAAACTCC. The following starter sequences were used: *rbcL* (gi|340511649) L: AGTATGGCCGTCCCCTATTG, R: TGATTTCACCTGTTTCGGCC, leaf catalase (*catL*) (gi|3202031) L: ACGCTCTTTCTGATCCTCGT, R: TTTCTGCCATGCTGTTTCTC, *pepc1* (TC8857) L: ACGCACCTGGGCATTGGGTC, R:AGGGCCAAACAAAGGGCGCT, *NADP-MDH* (TC4960) L: TCCTCAACCAGCCGATCTT, R: TCTTCACAGTGGAAGCACAGA, *cAPX1* (gi|4835908) L: TGCTTTCTTCCGTGACTACG, R: TAGCTCAGGATGACCACAGC

Reaction efficiency was tested by serial dilutions of cDNAs with gene specific primers. All samples were run in triplicates.

2.4. Chlorophyll fluorescence

Chlorophyll fluorescence measurements were performed 48 h post-inoculation (hpi) using Dual-PAM-100 (P700 & Chlorophyll Fluorescence Measuring System, Walz Mess- und Regeltechnik, Germany) according to the manual.

2.5. Carbon isotope analysis in organic samples

Frozen pooled samples made of leaf tissue of 5 plants were oven dried for 24 h at 105 °C before being ground to fine powder for isotopic analysis. Isotope ratio measurements of (^{13}C discrimination) were performed on a Finnigan MAT 253 Mass Spectrometer coupled with a Flash HT Elemental Analyzer in continuous flow mode.

2.6. Microscopic analysis

Hand-cut leaf cross sections were stained with 0.1% aniline blue in 1 M glycine, adjusted with NaOH to pH 9.4 up to 5 min. The sections were analyzed in 0.1 M glycine buffer by light and fluorescent microscopy using an Aristoplan epifluorescence microscope (Leica, Wetzlar Germany, with UV Filter Block A, and Orthomat E camera system).

2.7. Statistical analysis

The results were analyzed using Statistica 10 (Statsoft, USA) statistical software. One-way ANOVA followed by Tukey's HSD multiple range test were used to determine the individual treatment effects at $p \leq 0.05$.

3. Results

Observation of plant–pathogen interaction confirmed that the pathogen spread was restricted to necrotic lesions. In our studies such lesions never embraced mid-rib parts. Growth of spores germinating in close vicinity of mid-rib is usually restricted to the bundle sheath (Fig 1B).

We analyzed the expression of genes related to carbon and reactive oxygen species metabolism. All data were normalized in relation to C$_3$ plant mesophyll treated as control. In C$_3$ plants RubisCO, large subunit gene (*rbcL*) has shown significantly higher transcript abundance in mesophyll than in mid-rib parts. Similar differences were observed in CAM-performing leaves (Fig. 2A). Inoculation of leaf lamina induced no significant changes in C$_3$ leaves. While in CAM plants the mesophyll *rbcL* transcript level remained unchanged, a significant decrease was observed after inoculation in mid-ribs.

In C$_3$ plants, PEPC gene expression was found to be relatively low in both mesophyll and mid-rib parts, and inoculation induced no significant changes (Fig. 2B). The abundance of *pepc1* transcripts found in CAM plants confirmed that they perform β-carboxylation. Moreover, distinctively higher PEPC transcript abundance was found in mesophyll leaf parts. Infection significantly down-regulated the expression in both mesophyll and mid-rib parts.

NADP-ME is involved in both photosynthesis and the stress response. In C$_3$ plants, the abundance of NADP-ME message was relatively low and no substantial differences were shown between mesophyll and mid-ribs. The *nadpme1* transcript abundance did not change significantly after infection (Fig. 2C). In CAM-performing leaves, the expression of this gene was significantly higher, with distinctive differences between mesophyll and mid-rib parts. After infection, a significant increase and decrease of transcript abundance in mesophyll and mid-rib parts, respectively, was observed.
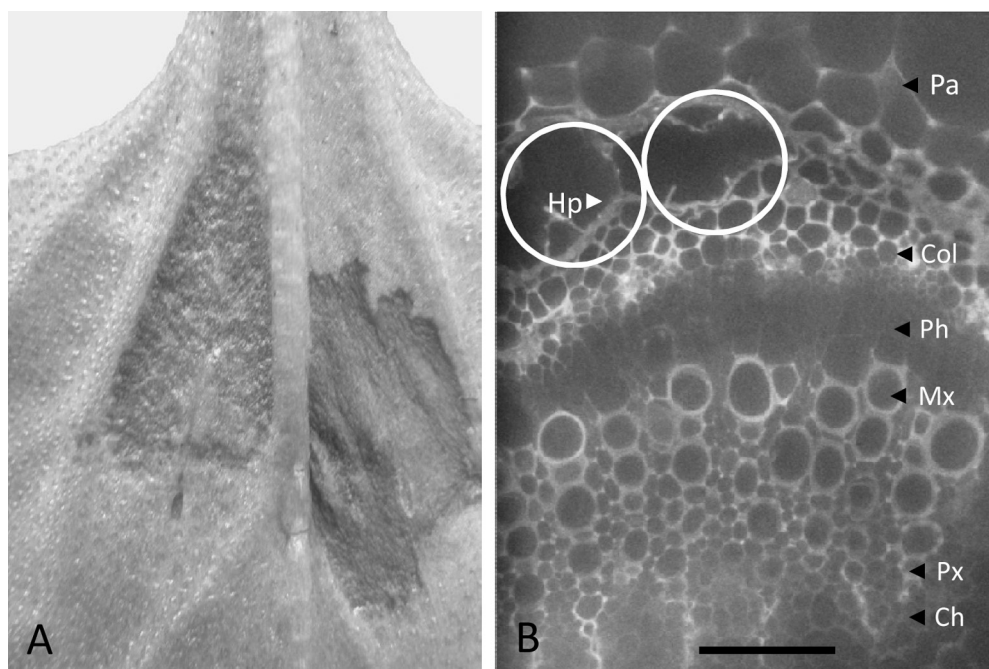
Fig. 1. Infection development in C_3 leaf of *Mesembryanthemum crystallinum* colonized by *Botrytis cinerea*. Abaxial leaf side 4 days post infection (A). Cross section of mid-rib and *B. cinerea* development in fluorescence microscopy (B); Px—protoxylem; Mx—metaxylem; Ph—phloem; Col—collenchyma; Pa—parenchyma; Ch—chloroplasts; Hp—hyphae. Scale bar = 100 μm.

Table 1

^{13}C discrimination in mesophyll (m) and mid-rib (v) leaf parts of intact *Mesembryanthemum crystallinum* plants performing C_3 and CAM photosynthesis. Similar tests were conducted 48 h post inoculation (hpi) of mesophyll with *Botrytis cinerea* spores on the same leaf parts (mesophyll—m INF, mid-rib—v INF).

Leaf part	δ^{13}C (‰)	
	C_3	CAM
m	−31.29 (±0.01)	−25.95 (±0.01)
v	−30.81 (±0.01)	−26.98 (±0.01)
m INF	−31.01 (±0.01)	−26.82 (±0.02)
v INF	−30.85 (±0.03)	−26.87 (±0.02)

We also quantified gene expression of proteins involved in ROS metabolism, catalase (*catL*) and cytosolic ascorbate peroxidase (*cAPX1*) in particular. In C_3 plants, mesophyll and mid-ribs varied distinctly in respect to *catL*. Significantly lower transcript abundance was found in the mid-rib parts (Fig. 3A). *B. cinerea* infection significantly changed *catL* transcript content. Expression of *catL* was decreased in mesophyll cells and the opposite reaction was shown for the mid-rib part. In CAM-performing plants, no significant differences between mesophyll and mid-rib parts were observed. Infection induced a substantial increase in *catL* transcript content in mesophyll and no significant changes in leaf mid-ribs were found.

We found no significant differences between *cAPX1* transcript abundance in C_3 mesophyll and mid-rib parts. *B. cinerea* did not alter gene expression, however, it substantially increased transcript abundance in the mid-rib parts. In CAM plants, significantly higher *cAPX1* gene transcript abundance was found in both leaf parts (Fig. 3B). Inoculation induced changes similar to those previously described for *nadpme1* and *catL*.

^{13}C discrimination studies have shown significant differences between C_3 and CAM plants. However, no distinctive differences between mesophyll and mid-rib leaf parts of both C_3 and CAM plants were found. Increase in ^{13}C value documents that salt treated experimental plant had shifted to CAM (Table 1).

Table 2

Chlorophyll *a* fluorescence parameters measured in intact mesophyll (m) and mid-rib (v) leaf parts of *Mesembryanthemum crystallinum* performing C_3 and CAM photosynthesis. Measurements were also performed 48 h post inoculation (hpi) (phase III of CAM) of leaf lamina with *Botrytis cinerea* spores in the area of mesophyll (m INF) and mid-ribs (v INF). ETR(I) and (II)—electron transport rate of photosystem I and II; NPQ—non photochemical quenching; Y(I) and (II)—yield of photosystem I and II.

	Leaf part	ETR(I)	ETR(II)	Y(I)	Y(II)	NPQ
C_3	m	21.6 a	14.9 a	0.872 a	0.832 ab	0.141 a
	v	22.8 a	12.8 a	0.918 a	0.822 ab	0.105 a
	m INF	22.6 a	13.7 a	0.912 a	0.791 bc	0.139 a
	v INF	24.8 a	12.5 a	1.000 a	0.792 abc	0.100 a
CAM	m	19.9 a	14.2 a	0.803 a	0.817 ab	0.161 a
	v	23.5 a	17.0 a	0.948 a	0.835 ab	0.133 a
	m INF	19.7 a	12.8 a	0.796 a	0.768 c	0.213 a
	v INF	17.7 a	16.5 a	0.712 a	0.838 a	0.168 a

Data were subjected to two-way ANOVA ($n = 2$). Means within a column followed by different letters are significantly different at $P < 0.05$ according to Tukey's HSD test.

Using chlorophyll *a* fluorescence, we estimated the photochemical activity of PSI and PSII (Table 2). No significant differences between mesophyll and mid-rib leaf parts were observed in the effective quantum yield of PSII (Y(II)), photochemical quantum yield PSI (Y(I)) or electron transport rates (ETR(I), ETR(II)) and non-photochemical quenching (NPQ). Infection induced no significant changes in C_3, and CAM plants, with the exception of Y(II) in the mesophyll of CAM leaves, where a significant decrease was shown.

4. Discussion

According to Fig. 1, germinating hyphae of *B. cinerea* easily penetrate the mesophyll tissue. They are capable of reaching the bundle sheath, but only occasionally invade the mid-ribs. We suggest that this may be related to high H_2O_2 concentrations in vascular parts of both C_3 and CAM plants, what beside tissue structure is probably the reason for restricted pathogen growth. Millimolar H_2O_2 concentrations can negatively affect *B. cinerea* growth, as were
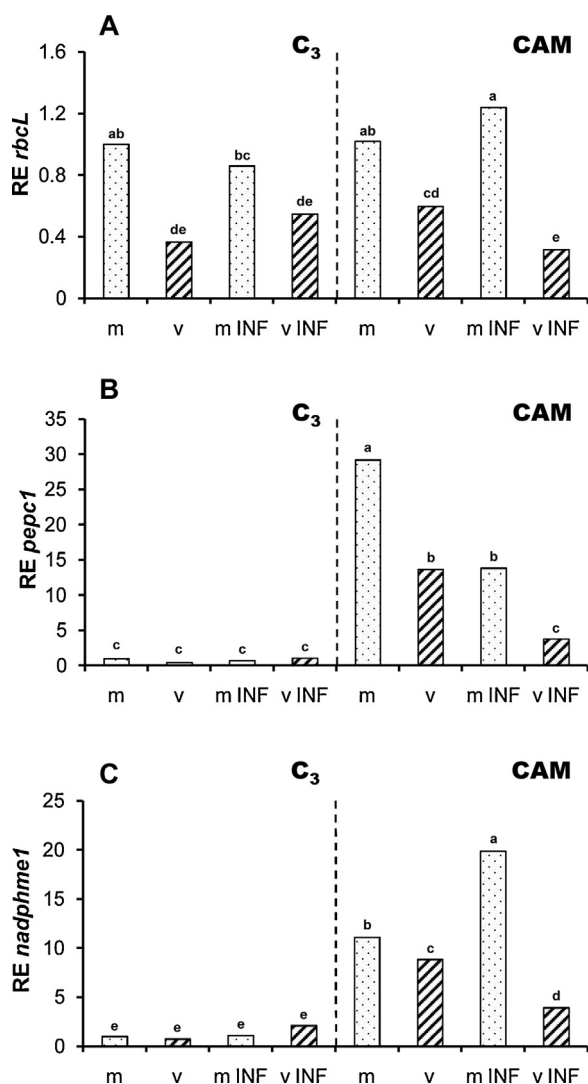
Fig. 2. Relative expression (RE) of photosynthetic genes, namely, large RubisCO subunit (*rbcL*) (A) phospho*enol*pyruvate carboxylase (*pepc1*) (B) and malic enzymes (*nadpme1*) (C) in mesophyll (m) and mid-rib (v) parts of intact *Mesembryanthemum crystallinum* leaves. Gene transcript levels were evaluated in indicated leaf parts (mesophyll—m INF, mid-rib—v INF) 48 h post inoculation (hpi) of leaf lamina with *Botrytis cinerea* spores. All values were calculated with Livak's procedure by comparison with C_3 mesophyll (value = 1.0). Bars represent mean values from 3 independent measurements. Different letters above bars indicate statistically significant differences in relation to control at $P \leq 0,05$ according to Tukey's (HSD) test.
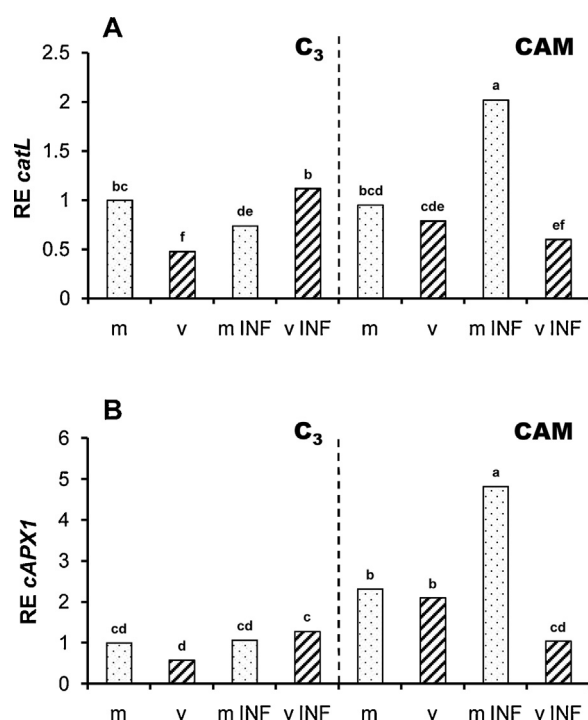

Fig. 3. Relative expression (RE) of antioxidative protein genes, namely, catalase (*catL*) (A) cytosolic ascorbate peroxidase (*cAPX1*) (B) in mesophyll (m) and mid-rib (v) parts of intact *Mesembryanthemum crystallinum* leaves. Gene transcript levels were evaluated in indicated leaf parts (mesophyll—m INF, mid-rib—v INF) 48 h post inoculation (hpi) of leaf lamina with *Botrytis cinerea* spores. All values were calculated with Livak's procedure by comparison to C_3 mesophyll (value = 1.0). Bars represent mean values from 3 independent measurements. Different letters above bars indicate statistically significant differences in relation to control at $P \leq 0,05$ according to Tukey's test.

described previously (Kuźniak et al., 2010). In line with this suggestion, the hyphae of *B. cinerea* were sporadically found in the xylem vessels of *M. crystallinum* leaves and exhibited clear symptoms of degeneration (Gabara et al., 2012).

In previous experiments on *M. crystallinum* we reported higher activity of NADP-ME (malic enzyme) in veins than in mesophyll in both C_3- and CAM-performing plants. We proposed that the leaf mid-ribs accumulate high quantities of H_2O_2 serving as a H_2O_2 reservoir that is utilized in various stress responses (Ślesak et al., 2008). ROS derived from the oxidative burst are mainly generated by the NAPDH-dependent oxidase D homolog (Mittler et al., 2011). It is the initial signal at the site of stress, triggering a ROS wave which activates various stress associated reactions. Activity of NADP-ME in leaf mid-ribs can supply plasma-membrane NADPH-dependent oxidases with cofactors, possibly leading to $O_2^{\bullet-}$ and H_2O_2 generation.

In *Nicotiana* sp. (C_3 plant) it was shown that carbon dioxide is delivered as malate and released by decarboxylation (with

NADP-ME) within the xylem and phloem (Hibberd and Quick, 2002). To confirm this molecularly, we analyzed the expression of photosynthesis-associated genes, namely *pepc1*, *rbcL*, *nadp-me1*. Our studies have shown that not only in mid-rib parts, but also in mesophyll of C_3 *M. crystallinum* leaves, the transcript abundance for both *pepc1* and *nadpme1* genes was significantly lower when compared with the same leaf parts of CAM plants. This indicates a different fixation mode of CO_2 in C_3 and CAM plants what was confirmed with ^{13}C discrimination (Table 1). This result unequivocally excluded intensive β-carboxylation or decarboxylation processes in mid-rib parts of C_3 plant leaves. Additionally, analysis of RubisCO's large subunit gene expression revealed a significant difference between mesophyll and mid-rib of C_3 plants probably emerging from the functional specificity of these leaf parts.

For the majority of photosynthetic genes, successful fungal infection results in a down-regulation of CO_2-fixating enzymes genes expression (RubisCO, PEPC) and photosystems I and II proteins (Bilgin et al., 2010). In our experiments, unaffected RubisCO expression in mesophyll of both C_3 and CAM plants may suggest that infection remained under the control of the plants which were able to sustain physiological rates of photosynthesis. It was confirmed with measurements of photochemical activity showing only insignificant changes due to infection (Table 2). However, in inoculated CAM-performing plants, mesophyll *nadpme1* was stimulated and *pepc1* inhibited. The latter result could support earlier observations suggesting inhibition of CAM-typical behavior due to infection (Kuźniak et al., 2010).

In C_3 plants we found distinctly lower abundance of *cAPX1* (however, not significant) and peroxisomal *catL* in mid-rib parts in comparison to mesophyll. Many studies confirmed that meso-

phyll cells are better prepared for respiratory function than bundle sheath cells (Robertson et al., 1995; Koroleva et al., 2000). It was also found that mesophyll cells have higher intrinsic capacity for photorespiration (more abundant P subunit of glycine decarboxylase) than bundle sheath cells (Tobin et al., 1991). All of these data suggest intensified ROS generation, not only from mitochondrial electron transport, but also from photorespiration in the mesophyll. On the other hand, both enzymes are potent H_2O_2 scavengers, thus, according to our expectations, their low expression in leaf mid-rib may support the concept of H_2O_2 reservoir in leaf veins.

In CAM plants infection of the lamina resulted in a significant *cAPX1* transcript increase in mesophyll and a simultaneous decrease in the mid-rib region. This result strongly indicates that carbon metabolism affects the direction of changes in the antioxidative machinery. In the mesophyll we also found high transcript levels of CAT. This was confirmed also on the level of protein activity (Libik-Konieczny et al., 2011). This allowed quick removal of ROS in the closest vicinity of the invading pathogen. On the other hand, low transcript level in the mid-rib part allow maintenance of elevated H_2O_2 concentration what refers to the mentioned function of H_2O_2 in mid-ribs.

Changes observed for *catL* and *cAPX1* transcripts in CAM plants were parallel to those in *nadpme1* expression. All three proteins may be regarded as stress enzymes induced *via* similar mechanisms, establishing high H_2O_2 concentrations in mid-ribs responsible for generation of systemic signals (Mittler et al., 2004). In CAM plants, NADP-ME action is usually connected with photosynthesis and decarboxylation. However, its increased expression in inoculated mesophyll had probably a different physiological meaning, especially when linked with parallel *pepc1* down-regulation. Up-regulated NADP-ME may suggest that the enzyme is properly supplied with its substrate; it can be alternatively supplied by the malate valve (Scheibe 2004) or from xylem and phloem (Hibberd and Quick, 2002). All of our results indicate that NADP-ME is a key enzyme required for establishing a local, as well as a systemic response to biotic stress.

5. Conclusions

That the expression of the large subunit of RubisCO is not affected by infection with *B. cinerea* in C$_3$ and CAM plants suggests a sustained photosynthesis rate, while a parallel down-regulation of *pepc1* in CAM tissues suggests at least partial inhibition of β-carboxylation. Up-regulation of NADP-ME expression upon infection confirms its essential role in stress response rather than in photosynthesis. This confirms earlier findings that CAM plants are more resistant to pathogen.

Acknowledgements

References

Bilgin, D., Zavala, J., Zhu, J., Clough, S., Ort, D., DeLucia, E., 2010. Plant Cell Environ. 33, 1597–1613.

Casati, P., Drincovich, M.F., Edwards, G.E., Andreo, C.S., 1999. Photosynth. Res. 61, 99–105.

Dodd, A., Borland, A., Haslam, R., Griffiths, H., Maxwell, K., 2002. J. Exp. Bot. 53, 569–580.

Gabara, B., Kuźniak, E., Skłodowska, M., Surówka, E., Miszalski, Z., 2012. Environ. Exp. Bot. 77, 33–43.

Gorecka, M., Alvarez-Fernandez, R., Slattery, K., McAusland, L., Davey, P., Karpinski, S., et al., 2015. Philos. T. R. Soc. B 369, 20130234.

Hibberd, J.M., Quick, W.P., 2002. Nature 415, 451–454.

Karpinski, S., Reynolds, H., Karpinska, B., Wingsle, G., Creissen, G., Mullineaux, P., 1999. Science 284, 654–657.

Kocurek, M., Kornas, A., Pilarski, J., Tokarz, K., Lüttge, U., Miszalski, Z., 2015. Trees, http://dx.doi.org/10.1007/s00468-015-1182-7

Koroleva, O.A., Tomos, A.D., Farrar, J., Roberts, P., Pollock, C.J., 2000. Aust. J. Plant Physiol. 27, 747–755.

Kuźniak, E., Kornas, A., Gabara, B., Ullrich, C., Skłodowska, M., Miszalski, Z., 2010. Environ. Exp. Bot. 69, 137–147.

Kuźniak, E., Gabara, B., Skłodowska, M., Libik-Konieczny, M., Miszalski, Z., 2011. Biol. Plant. 55, 423–430.

Libik-Konieczny, M., Surówka, E., Kuźniak, E., Nosek, M., Miszalski, Z., 2011. J. Plant Physiol. 168, 1052–1059.

Libik-Konieczny, M., Surówka, E., Nosek, M., Goraj, S., Miszalski, Z., 2012. Acta Physiol. Plant. 34, 1471–1477.

Leegood, R.C., 2008. J. Exp. Bot. 59, 1663–1673.

Lüttge, U., 2004. Ann. Bot. 93, 629–652.

Mittler, R., Vanderauwera, S., Suzuki, N., Miller, G., Tognetti, V.B., Vandepoele, K., et al., 2011. Trends Plant Sci. 16, 1360–1385.

Miszalski, Z., Kluge, M., Ziegler, H., 1997. J. Plant Physiol. 151, 535–540.

Mittler, R., Vanderauwera, S., Gollery, M., Van Breusegem, F., 2004. Trends Plant Sci. 9, 490–498.

Robertson, E.J., Williams, M., Harwood, J.L., Lindsay, G., Leaver, C.J., Leech, R.M., 1995. Plant Physiol. 108, 469–474.

Sage, R.F., 2004. New Phytol. 161, 341–370.

Scheibe, R., 2004. Physiol. Plant. 120, 21–26.

Ślesak, I., Ślesak, H., Libik, M., Miszalski, Z., 2008. J. Plant Physiol. 165, 127–137.

Szechyńska-Hebda, M., Kruk, J., Górecka, M., Karpińska, B., Karpiński, S., 2010. Plant Cell 22, 2201–2218.

Tobin, A.K., Thorpe, J.R., Hylton, C.M., Rawsthorne, S., 1991. Plant Physiol. 91, 1219–1225.